Harnessing the power of microfluidics in sustainable sonochemistry: case study of ultra-fast removal of methyl orange from wastewater.

Quang Thang Trinh[1,#,*], Yuran Cheng[1,2,#], Haotian Cha[1,#], Kin Un Tai[1], Lingxi Ouyang[1], Prince Nana Amaniampong[3], Jun Zhang[1], Hongjie An[1], Zuojun Wei[2,*], Nam-Trung Nguyen[1,*]

[1] *Queensland Micro and Nanotechnology Centre, Griffith University, 4111, Kessel Road, Queensland, Australia.*

[2] *Key Laboratory of Biomass Chemical Engineering of the Ministry of Education, College of Chemical and Biological Engineering, Zhejiang University, Hangzhou, Zhejiang, 310058, P.R. China.*

[3] *Institut de Chimie des Milieux et Matériaux de Poitiers, CNRS, Université de Poitiers ; 1 rue Marcel Doré, Bat B1 (ENSI-Poitiers), 86073 Poitiers, France.*

*** Corresponding authors:**

Email: q.trinh@griffith.edu.au (Q.T.T.)
Weizuojun@zju.edu.cn (Z.W.)
nam-trung.nguyen@griffith.edu.au (N.-T.N)

[#] Quang Thang Trinh, Yuran Cheng and Haotian Cha contributed equally to this work.

Abstract.

The oxidation of renewable resources is a promising process that has great potential in addressing the climate change and building the circular economic, sustainable society and green chemical supply chain. This study explores the application of ultrasound in oxidation processes using the wastewater treatment as a case study. Advanced oxidation processes (AOPs) are highly effective for degrading the pollutants in wastewater through the generation of oxidative radicals, with ultrasound emerging as a promising AOP method due to its mild conditions and synergistic potential with other methods. However, ultrasound alone faces challenges in efficiently degrading complex compounds like azo dyes, partly due to issues with cavitation bubble stability and non-uniform ultrasonic fields. Microfluidic reactor combined with microbubble technology offers a solution to enhance ultrasound efficiency by improving bubble stability and energy distribution. In this study, we investigate microbubble formation in a microfluidic reactor with T-junction and flow-focusing inlets, aiming to enhance ultrasound-driven AOPs. The flow-focusing design successfully generates relatively small and monodisperse bubbles allowing for effective ultrasound application at 108.5 kHz using a piezoelectric transducer. Our results demonstrate a relatively high H_2O_2 generation rate of 0.54 μM/s, among the highest reported in the literature, and a methyl orange (MO) degradation efficiency of 35% in just 2.9 seconds - significantly surpassing conventional systems and prior microfluidic studies. This work demonstrates the novelty of integrating microbubble technology with microfluidic reactors to enhance the energy efficiency of ultrasound - assisted oxidation processes, providing an efficient approach to the chemo-selective conversion of renewable resources to high-value specialty chemicals that are inaccessible via conventional routes.

Keywords. Wastewater treatment, Sonochemistry, Advanced oxidation processes (AOPs), Cavitation, Microfluidics, Microbubbles, Methyl orange.

1. Introduction

The United Nations estimates that the world population will grow to 9.8 billion by 2050. This population inflation will drastically increase the demand for clean water, energy, food, and chemicals. Sustainably meeting these demands while protecting our environment has become a priority, in line with the United Nations Sustainable Development Goals. In this context, chemistry plays an important role in addressing the challenge: ***"how to produce more chemicals while minimising detrimental impacts on environment and society".*** The progressive incorporation of renewable biomass resources, including carbohydrates, lignin, polysaccharides, in the chemical industry is a game changing transition towards building a circular and sustainable chemical supply chain. This contribution is driven by their carbon-neutral nature and the massive capacity in producing a wide range of fuels and chemicals. However, controlling the selective conversion of these polyfunctional substrates is a grand challenge, which is currently limiting the great potential of biomass transformation to high-value specialty chemicals such as bio-based products. Simply tuning temperature does not enable exquisite control of reaction selectivity, thus, new technologies are needed. To address this selectivity challenge, a new concept of assisted catalysis has emerged wherein chemical reactions are driven at room temperature by external triggers like electrical potentials, photons, plasmons, and ultrasound.

Among these driving forces, ultrasound is witnessing a renaissance. When ultrasonic waves propagate in a liquid, they change the density of the fluid and with sufficient acoustic intensity, these waves disrupt the tensile forces of the liquid, creating micro-sized cavitation bubbles. Cavitation events are accompanied by sudden increases in local pressure (up to several MPa) and local temperature (up to thousands of °C). The effect of cavitation bubbles collapsing (or imploding) in a liquid depends on the applied frequency. For instance, Low Frequency Ultrasound (LFUS) (20-80 kHz) generates small quantities of large cavitation bubbles (~170 μm at 20 kHz). The bubble collapse mainly induces physical effects such as shock waves, high speed jets, etc. Therefore, LFUS is used for the erosion/deagglomeration

of particles, breaking long chain polymers, etc. In contrast, High Frequency Ultrasound (HFUS, > 100 kHz) generates large number of small sized cavitation bubbles. The implosion of these bubbles, which is substantially accelerated by the inertia of the surrounding fluid (inertial cavitation), propels radicals into the bulk solution. These ultrasound-generated radicals can participate in chemical reactions and are highly effective in the oxidation of aqueous pollutants in wastewater.

Wastewater treatment is a crucial environmental challenge, as industrial effluents from textile, pharmaceutical, and agricultural sources often contain organic chemicals, leading to serious environmental and health issues. Current wastewater remediation strategies include biotreatment, membrane separation, microbial electrochemical systems, adsorption and advanced oxidation processes (AOPs) (Sivanesan et al. 2024). Among these strategies, AOPs are particularly effective for degrading persistent organic pollutants due to their ability of in situ generation of highly oxidative radical species (Wang and Wang 2020). Advanced oxidation processes encompass a variety of methods, such as Fenton reactions, photocatalysis, ozonation, electrocatalysis, and ultrasound (Fedorov et al. 2022). Ultrasound, in particular, has emerged as a promising AOP due to its mild operating conditions, absence of chemical additives, and synergistic enhancement when used alongside other treatment methods (Rayaroth et al. 2016). The fundamental mechanism of ultrasound in AOPs is based on the phenomenon of acoustic cavitation, where rapid bubble expansion and collapse generate localized extreme temperatures and pressures, leading to the formation of hydroxyl (•OH) and hydrogen (•H) radicals that effectively degrade organic pollutants (Cintas and Luche 1999).

However, despite its potential, ultrasound treatment faces challenges, especially when applied to recalcitrant nitrogen-containing compounds (Rayaroth et al. 2022, Shanker et al. 2017). These compounds are commonly found in industrial wastewater, and current studies show limited degradation efficiency for complex azo molecules like methyl orange (MO) when using ultrasound alone, with typical removal rates falling below 10% (Cheng et al. 2012, Yuan et al. 2016). One reason for this low efficiency is the

coalescence and rapid degassing of cavitation bubbles, which reduces their number and persistence (Yusuf et al. 2024). Besides, conventional bulk ultrasound systems, often employing simple sonicators, typically suffer from non-uniform ultrasonic fields and require high power over long duration to achieve moderate removal rates. Hybrid methods, which combine ultrasound with other processes like photocatalysis or ozonation, can improve degradation rates but come with drawbacks, such as the need for additional catalysts, oxidants, and precisely controlled equipment (Amaniampong et al. 2024, Lee et al. 2023, Li et al. 2023b).

To overcome these limitations, microfluidic reactors offer a promising alternative by allowing precise control over mass and heat transfer, as well as improving the mixing process of liquid and gas phases (Cordier et al. 2023, Li et al. 2023a, Volk et al. 2020). Recent study has shown the advantages of ultrasound in a microfluidic chip, achieving a 9% removal rate in just 36 seconds due to uniform ultrasound distribution and efficient energy transfer (Thangavadivel et al. 2014). Moreover, microbubble technology, known for its high surface-area-to-volume ratio and enhanced mass transfer, has shown the potential to increase hydroxyl radical production during acoustic cavitation (He et al. 2023, Janiak et al. 2023, Ma et al. 2020, Xiu et al. 2023). Stable microbubble formation within microfluidic reactors could further improve ultrasound-driven AOP efficiency by promoting sustained cavitation and enhancing radical generation (Rickel et al. 2018, Wan et al. 2008).

In this study, we investigate the synergy of microfluidics and sonochemistry, using the methyl orange degradation in wastewater treatment as a case study to assess the efficiency of this approach in oxidation processes. We firstly optimise the operation parameters of the new micro-sono-reactor with flow focusing design on the MO degradation. Next, we evaluate the formation of microbubbles in the newly designed flow-focusing microfluidic reactor and compare with the conventional reported T-junction microfluidic reactor in literature. We assess the sonochemical efficiency of those microfluidic sonoreactors via the generation rate of H_2O_2 driven by the microbubbles cavitation. Density Functional Theory (DFT)

calculations are performed to explain the mechanism of MO degradation under ultrasound conditions. The role of surfactant to the MO degradation efficiency is also conducted.

2. Methods.

2.1. Materials

All chemicals (Sigma-Aldrich) were used without further purification, including 30% H_2O_2 solution, methyl orange, $(NH_4)_6Mo_7O_{24}\cdot 4H_2O$, KI, $NaH_2PO_4\cdot H_2O$, $Na_2HPO_4\cdot 7H_2O$, $KMnO_4$, (3-Aminopropyl)-triethoxysilane (APTES), Acetone, Isopropanol, Methanol, Tween 20, PDMS, curing agent, NaOH.

2.2. Design and fabrication of microfluidic chips

In this study, we tested two designs of microfluidic sono-reactor to generate microbubbles. The first one had the flow focusing setup (Figure 1a) and was used as the main sonoreactor for MO degradation. The second one was the T-junction design with an intensive cavitation effect which had already reported by Tadiono et al. and was used as a reference in our study (Figure 1a). The main dimension of T-junction channel with 500 μm width, the width of side outlet is 200um. The height of the channel is 100 μm. The dimensions of the flow focusing channel are 30 μm in constriction width, 100 μm in width, 400 μm in spiral width, and 120 μm in height.

The microfluidics channel was fabricated using standard photolithography and soft-lithography technologies. Briefly, polydimethylsiloxane (PDMS) mixture was made using SYLGARDTM 184 (Dow Corning) silicone elastomer base was mixed 10: 1 with SYLGARDTM 184 silicone elastomer curing agent. Next, the mixture was placed in a vacuum chamber for 20 mins for degassing before being poured over the microchannel silicon mold, and then placed in an oven at 70 °C for over 2 hours. After being peeled from the mold, the inlet and outlet holes were punched with an 1-mm hole puncher. Finally, the PDMS layer was bonded to a glass substrate using Plasma Cleaner (Harrick Plasma). Tubing was attached to the inlet and outlet of the channel. The inlet tubing was further attached to a syringe pump. To maintain

the hydrophilicity of the microfluidic chip, the chip was treated in a freshly prepared 2% APTES solution in acetone for 15 minutes at room temperature after bonding, followed by rinsing with acetone and Milli-Q water (Siddique et al. 2017).

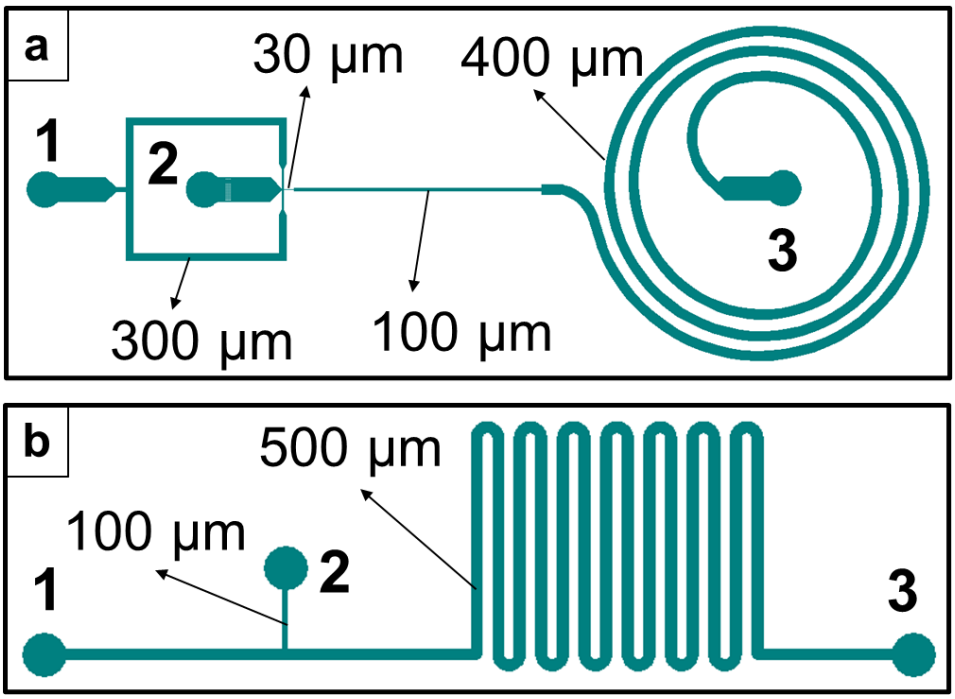

Figure 1. Two designs of microfluidic sonoreactor. (a) Flow focusing design. (b) T-function design.

2.3. Experimental setup

After obtaining the chips, the microfluidic sonoreactor was fabricated by securing a PZT-5H piezoelectric ceramic disc (20 × 2.1 mm, model SMD20T21F1000R; Steiner & Martins, Inc.) 5 mm from the spiral channel using epoxy resin. This piezoelectric ceramic disc was driven by a power amplifier (AG 1017L; T&C Power, Inc.) to generate ultrasound at a frequency of 108.5 kHz in radial vibration mode. The supplied power was adjusted to find the optimized operating conditions.

The microfluidic sonoreactor was placed on the stage of an inverted microscope (Olympus IX73 microscope). Two syringe pumps (SHENCHEN ISPLab02) were used to infuse the solution into the microfluidic device at distinct flow rates. All syringes employed in this setup were HAMILTON glass syringes. One syringe filled with the solution and the other left empty to serve as an air injection line. The experimental setup scheme is presented in Figure 2. By adjusting the flow rate ratio of air to solution, we

generated uniform bubbles within the microchannel. The formation, size and stability of the bubble were observed under the microscope. We evaluated the H_2O_2 concentration of effluent from T-junction and a flow-focusing microfluidic reactor to demonstrate the enhancement of microbubble in the acoustic cavitation. For the MO degradation experiment, all conditions remained the same, except that water was replaced with a MO solution of known concentration (typically 5 mg/L).

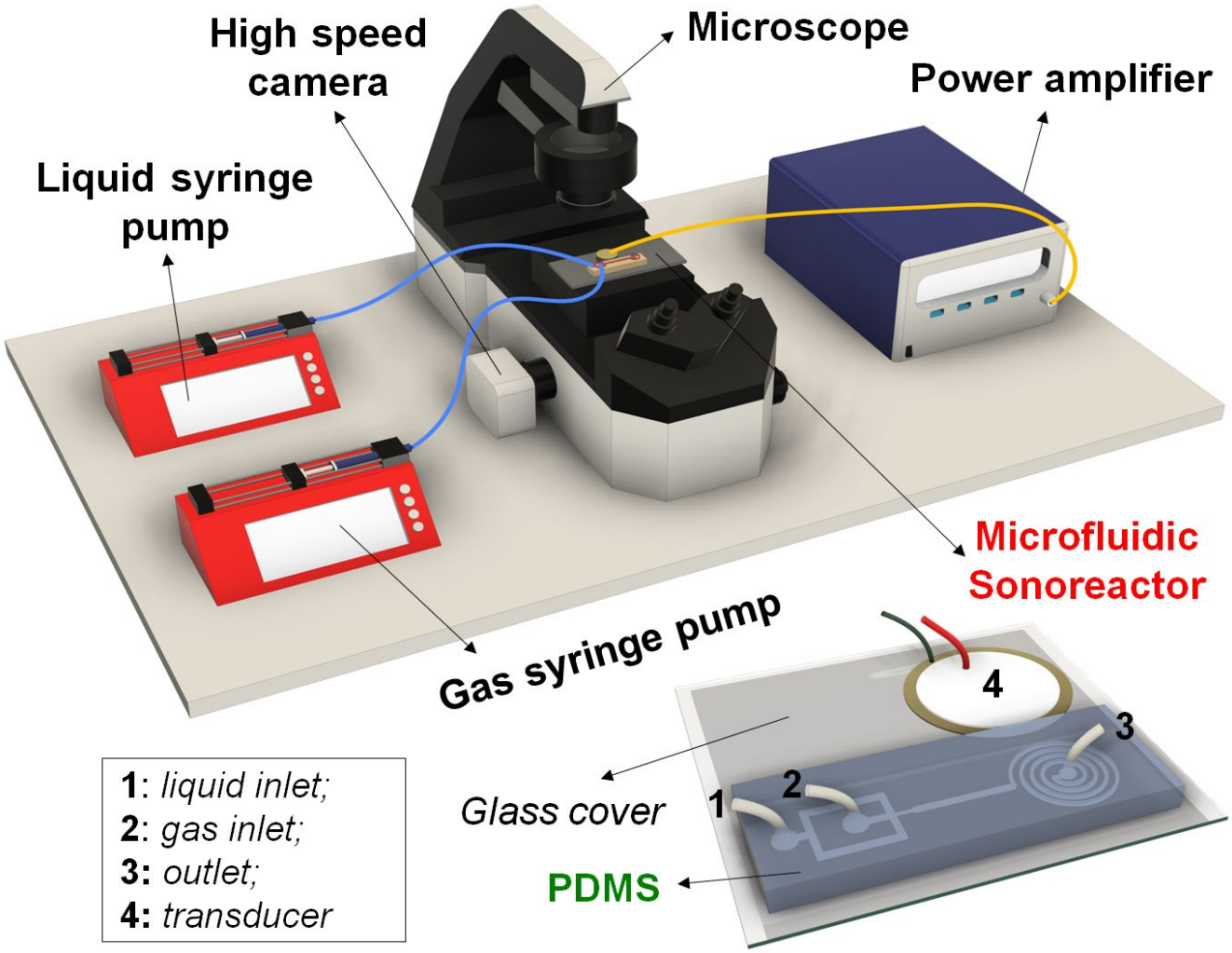

Figure 2. Experimental setup for the ultrasound-assisted degradation of methyl orange (MO) in a microfluidic sonoreactor.

2.4. Analytical methods

The generation of H_2O_2 was measured using I^{3-} spectrophotometric method reported in the literature (Xiao et al. 2019). 0.5 M phosphate buffer stock solutions with pH 4.5 was prepared by dissolving 1.3790 g $NaH_2PO_4 \cdot H_2O$ and 0.0026 g $Na_2HPO_4 \cdot 7H_2O$ in 100 mL Milli-Q water. 35 mM Mo(VI) solution was obtained by dissolving 0.0618 g $(NH_4)_6Mo_7O_{24} \cdot 4H_2O$ in 10 mL Milli-Q water. 1.2 M KI solution was

prepared by dissolving 19.92 g KI in 100 mL Milli-Q water. The three solutions were mixed in a 27:1:2 ratio to create a working solution, which was stored in dark conditions. For each test, 200 µL of the water sample was mixed with 300 µL of the working solution in a 1-cm Micro Quartz Cuvette, shaken in the dark for 30 seconds, and the absorbance at 350 nm was recorded using a UV-Vis spectrophotometer. The concentration of H_2O_2 in the 30% H_2O_2 solution was titrated as 9.72 M using a standard $KMnO_4$ solution. The calibration curve was established by diluting the 30% H_2O_2 solution to different concentrations (1, 5, 10, 50, 100µM). MO degradation was measured based on the absorbance at 465 nm using UV-Vis spectrophotometry. The calibration curve was established by MO solutions of known concentrations (1, 2, 3.2, 5, 7,10 mg/L).

2.5. DFT description

All spin polarized Density Functional Theory (DFT) calculations were performed with the VASP package using the projector augmented wave (PAW) method (Kresse and Furthmüller 1996, Kresse and Hafner 1993). Total energies were calculated using a plane wave energy cut-off of 500 eV, with the Perdew-Burke-Ernzerhof (PBE) exchange-correlation functional (Perdew et al. 1996). Total energies were computed using convergence thresholds of 10^{-5} eV for self-consistent field cycles, and a force threshold of 0.02 eV/Å. The force was minimized using the conjugate-gradient method. Dispersion correction was applied using the Grimme's D3 approach (Grimme et al. 2010). Gas phase species are optimized in a cubic unit cell size of 20×20×20 Å in vacuum and the Brillouin zone was sampled using a 1×1×1 Monkhorst–Pack k-point grid density (Monkhorst and Pack 1976).

3. Results and discussion

3.1. Methyl Orange degradation in a microfluidic sonoreactor

First, we investigated the influence of operation parameters to the performance of the microfluidic sonoreactor in MO degradation. We varied the total flow rate (of liquid and gas), gas-to-liquid flow ratio

and the applied power. In each case, only the parameter under investigation was allowed to change while other parameters were fixed. Figure 3 presents the experimental results.

In Figure 3a, we observed the optimized total flow rate of 120 μL/min. The higher the flow rate, the shorter the MO solution was exposed to ultrasound, resulting in the reduction of MO degradation efficiency. On the other hand, the lower the flow rate resulted in bubble coalescence when microbubbles travelled through the microchannel, reducing the cavitation magnitude and consequently decreased the MO degradation efficiency. Therefore, an optimum value exists for the total flow rate to achieve the highest MO degradation yield.

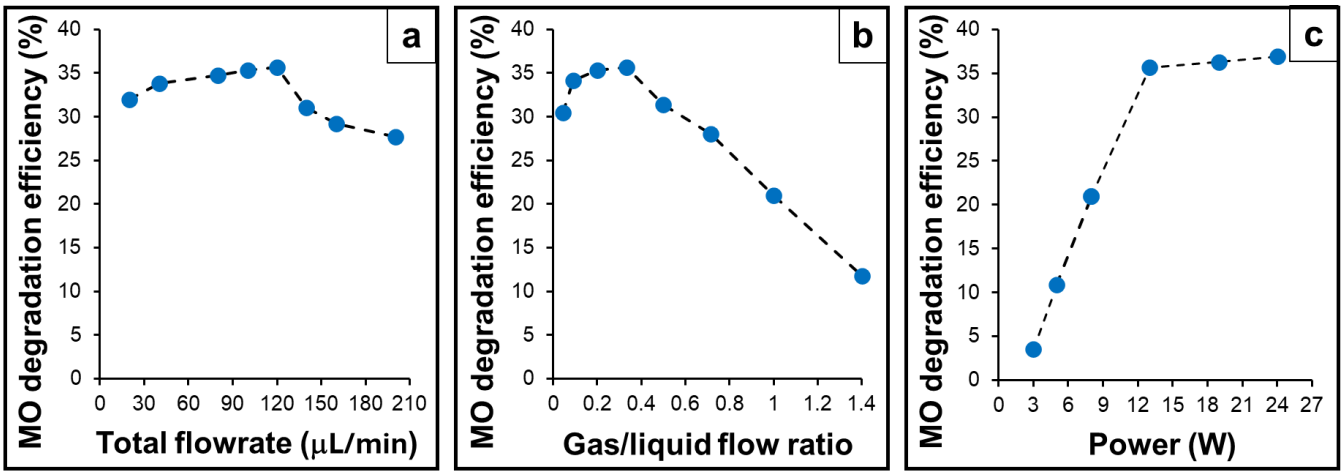

Figure 3. Influence of (a) total flow rate; (b) gas-to-liquid flow ratio and (c) applied power to the ultrasound-assisted MO degradation efficiency.

In Figure 3b, the optimized gas-to-liquid flow ratio of 1:3 resulted in the best performance of ultrasound-assisted MO degradation. The lower this gas-to-liquid flow ratio, the less microbubbles were generated, and the lower was the MO degradation efficiency. The higher the gas-to-liquid flow ratio, the larger bubbles were formed. Since the cavitation were detected to be occurred at the interface of gas/liquid, the interfacial area between liquid and gas varied inversely with the size of the bubbles. Therefore, large bubbles also resulted in a lower MO degradation efficiency. Finally, the influence of applied power to MO degradation efficiency is shown in Figure 3c. Low power (less than 13W) was not enough to induce strong cavitation that is essential for MO degradation. When the applied power was

stronger than 13W, the supplied power was lost to thermal energy, as was presented in a review by Trinh et al. Therefore, it explained the best-chosen power of 13W.

3.2. Sonochemical efficiency.

One grand challenge with ultrasound assisted degradation of organic pollutant in wastewater is the low energy efficiency of conventional sonochemical processes. Usually, the sonoreactor need extremely strong ultrasound power to generate a density of reactive oxygen species (ROS) high enough for the degradation. We showed that the microfluidic sonoreactors developed in this study have much better energy efficiency than almost other research in literature.

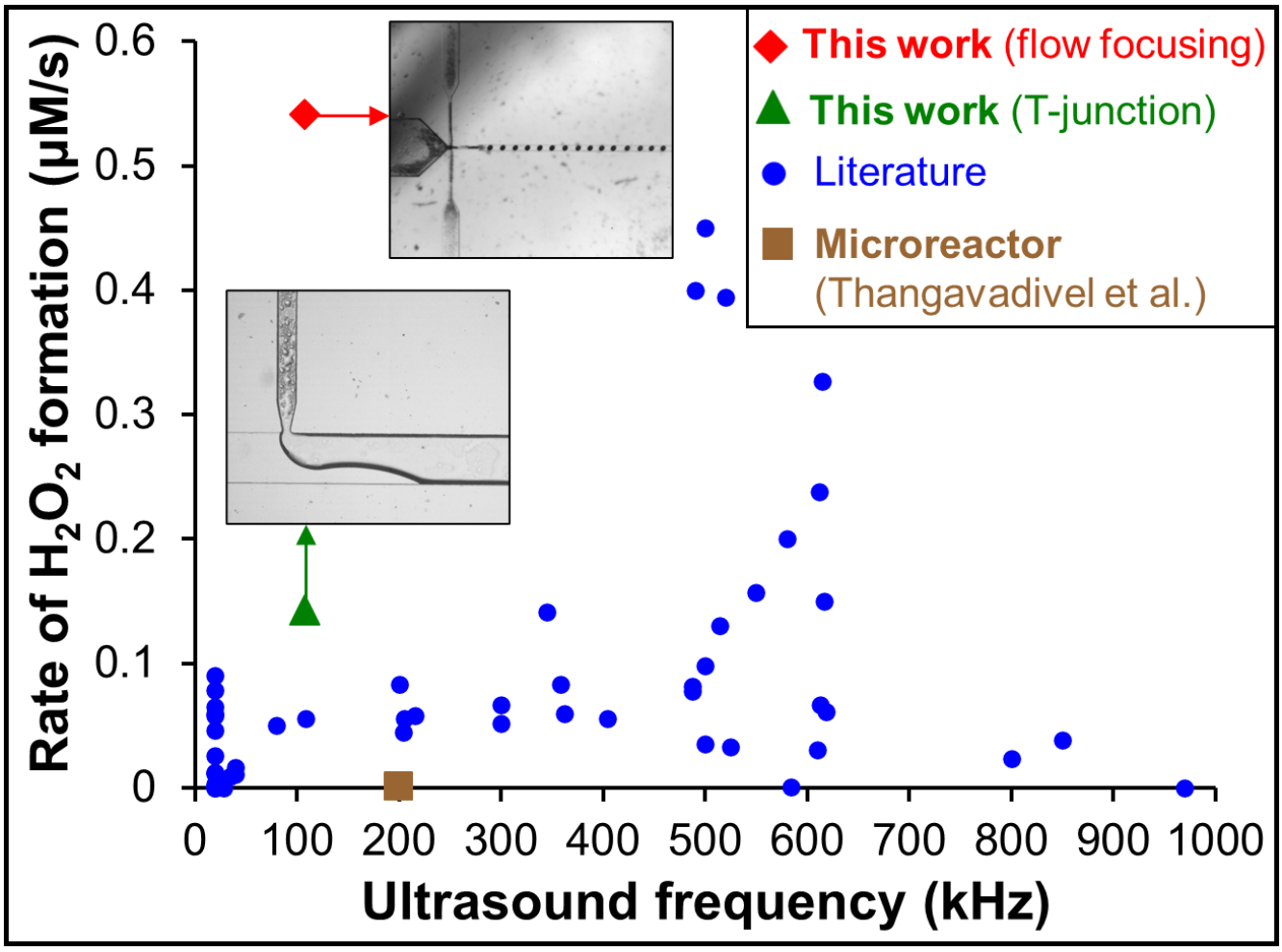

Figure 4. The rate of H_2O_2 formation (μM/min) achieved in the flow-focusing and T-junction microfluidic sonoreactors and are benchmarked with data in literature. Inserted images are the gas-liquid mixing and generation of microbubbles in the flow-focusing and T-junction microfluidic sonoreactors.

The energy efficiency is usually expressed in the capability to generate the OH radical, which could be detected via the formation rate of H_2O_2 by KI dosimetry method. The results presented in Figure 4

showed that the H_2O_2 formation rate in the flow-focusing sonoreactor was much higher than those reported in current literature. Interestingly, the T-junction sonoreactor, reported by Tadiono et al. only produced H_2O_2 with one-third rate slower than the flow-focusing sonoreactor. These data clearly demonstrated the great potential of carry out the degradation of organic pollutant in wastewater in the appropriately designed microfluidic sonoreactor.

3.3. Role of surfactant to the ultrasound-assisted MO degradation

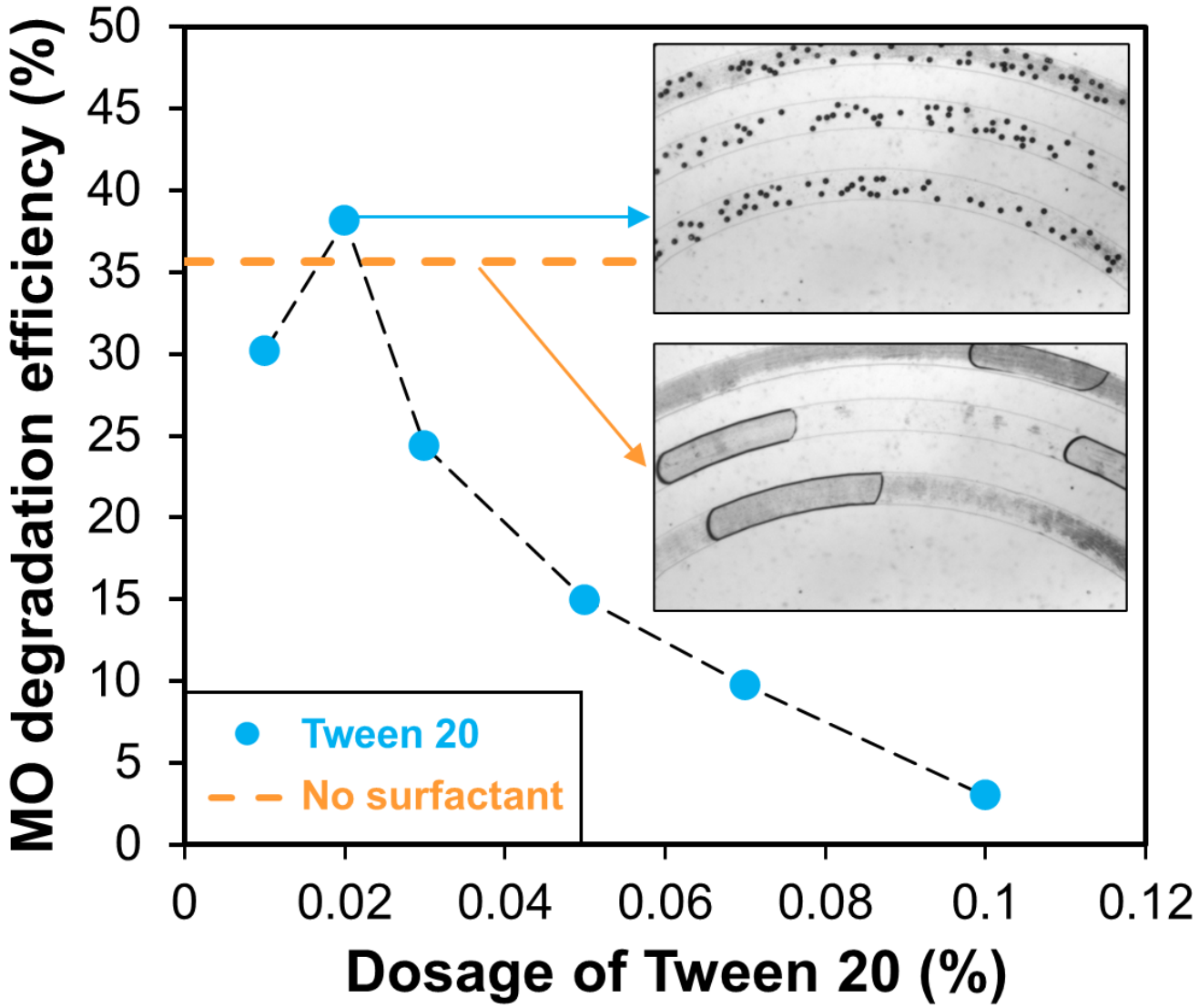

Figure 5. The influence of surfactant dosage to the MO degrdation efficiency. Inserted images are the formation of microbubbles in the flow-focusing microfluidic sonoreactor with and without the introduction of surfactant (Tween 20). Dash line represents the MO degradation efficiency without the presence of surfactant.

The role of surfactant to the sonochemical reactions is complicated. Two opposite roles of surfactant to the cavitation could be observed. The presence of surfactant induced the formation of smaller

microbubbles, forming high density of microbubbles (Figure 5). On the other hand, the surfactant also stabilized the microbubbles and made the cavitation more difficult. Therefore, there exits an optimum dosage of surfactant that gave the best MO degradation efficiency. According to Fig. 5, we obtained the best dosage of Tween 20 of 0.02%. At this dosage, the MO degradation efficiency is 38.1%, better than the value of 35.6% obtained without the presence of surfactant. It should be mentioned that the critical micelle concentration of Tween 20 is 0.06–0.07% in water at room temperature. The higher dosage than this range therefore does not have any positive effect to the formation of microbubbles, as is reflected by the low efficiency of 0.1% Tween 20 in Fig. 5.

3.4. DFT mechanism

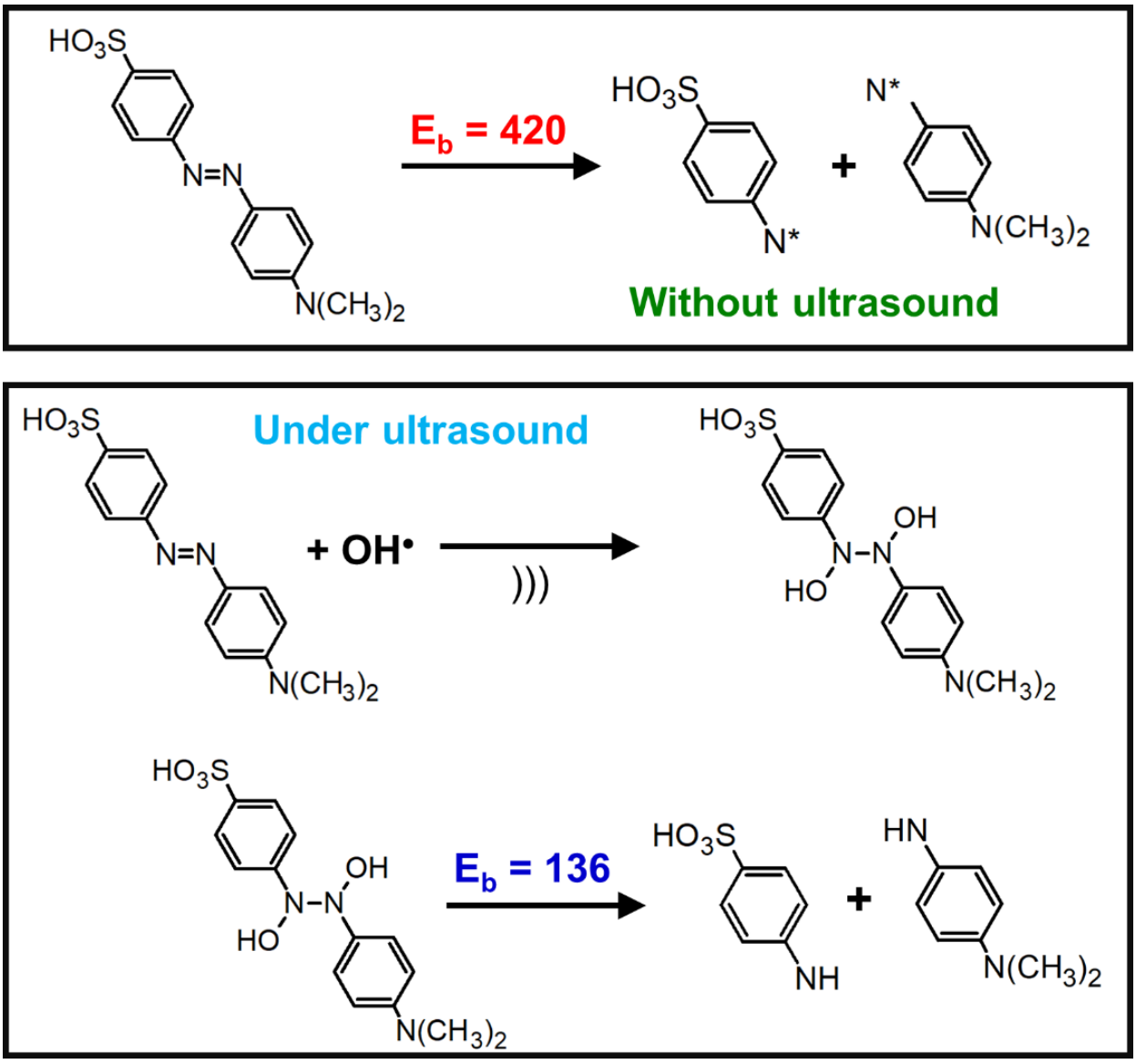

Figure 6. The activation of MO without and under ultrasound conditions

Density Functional Theory (DFT) calculations were performed to explain the role of ROS in activating MO. The key step for the degradation of MO is widely proposed to be the scission or the N=N bond, followed by the subsequent ring opening to smaller fragments (Lee et al. 2016, Lughmani et al. 2022, Sun et al. 2020, Xie et al. 2016). Without the ultrasound conditions, the DFT results show that the energy of the N=N bond in the MO molecule is ~420 kJ/mol, and therefore its cleavage is challenging. Under ultrasound conditions, the generation of OH species from the cavitation could facilitate an alternative pathway for the N=N bond dissociation. Indeed, we computed that the generated OH species could oxidize the N atoms on MO to the diazenediol derivative (also called as azanone dimer derivative or hyponitrous derivative), Figure 6. Once the diazenediol derivative was formed, the bond energy of R-OHN-NOH-R is significantly reduced to ~136 kJ/mol. It therefore explains the ability of MO to be degraded under ultrasound irradiation and again emphasize the need to design the microfluidic sonoreactor to optimise the sonochemical yield of producing highly active OH species.

4. Conclusion

This study demonstrates that combining microbubble technology with microfluidic reactors significantly enhances ultrasound-driven advanced oxidation processes (AOPs) for wastewater treatment. Using a flow-focusing sonoreactor, we achieved a high H_2O_2 generation rate of 0.54 μM/s and an exceptional 35% degradation efficiency for methyl orange in just 2.9 seconds. These outstanding results obtained in this study significantly surpass previous reports in a microfluidic system and those using additional catalysts (Table S1), highlighting the effectiveness of microbubbles and microfluidics in ultrasound AOP method. This study also illustrates a "proof-of-concept" for a novel and efficient approach to facilitate the selective oxidation of renewable resources to high-value specialty chemicals using the integration of microfluidics and sonochemistry.

Acknowledgement.

This work is financially supported by the Australian Research Council (FL230100023). Y.C. acknowledges financial support from the Zhejiang University Luk's Scholarship for Graduates International Exchange for the cooperation research conducted at Griffith University.

Conflict of interest. The authors have no relevant financial or nonfinancial interests to disclose.

Reference

Amaniampong, P.N., Mahendran, V., Trinh, Q.T., Zhangyue, X., Jonnalagadda, U., Gould, T., Nguyen, N.T., Kwan, J., Choksi, T., Liu, W., Valange, S. and Jerome, F. (2024) Localized Oxidative Catalytic Reactions Triggered by Cavitation Bubbles Confinement on Copper Oxide Microstructured Particles. Angew Chem Int Ed Engl, e202416543.

Cheng, Z., Quan, X., Xiong, Y., Yang, L. and Huang, Y. (2012) Synergistic degradation of methyl orange in an ultrasound intensified photocatalytic reactor. Ultrason Sonochem 19(5), 1027-1032.

Cintas, P. and Luche, J.L. (1999) Green chemistry - The sonochemical approach. Green Chemistry 1(3), 115-125.

Cordier, A., Klinksiek, M., Held, C., Legros, J. and Leveneur, S. (2023) Biocatalyst and continuous microfluidic reactor for an intensified production of n-butyl levulinate: Kinetic model assessment. Chemical Engineering Journal 451, 138541.

Fedorov, K., Dinesh, K., Sun, X., Soltani, R.D.C., Wang, Z.H., Sonawane, S. and Boczkaj, G. (2022) Synergistic effects of hybrid advanced oxidation processes (AOPs) based on hydrodynamic cavitation phenomenon - A review. Chemical Engineering Journal 432, 134191.

Grimme, S., Antony, J., Ehrlich, S. and Krieg, H. (2010) A consistent and accurate ab initio parametrization of density functional dispersion correction (DFT-D) for the 94 elements H-Pu. The Journal of Chemical Physics 132(15).

He, Y., Zhang, T., Lv, L., Tang, W., Wang, Y., Zhou, J. and Tang, S. (2023) Application of microbubbles in chemistry, wastewater treatment, medicine, cosmetics, and agriculture: a review. Environmental Chemistry Letters 21(6), 3245-3271.

Janiak, J., Li, Y., Ferry, Y., Doinikov, A.A. and Ahmed, D. (2023) Acoustic microbubble propulsion, train-like assembly and cargo transport. Nat Commun 14(1), 4705.

Kresse, G. and Furthmüller, J. (1996) Efficiency of ab-initio total energy calculations for metals and semiconductors using a plane-wave basis set. Computational Materials Science 6(1), 15-50.

Kresse, G. and Hafner, J. (1993) Ab initio molecular dynamics for liquid metals. Physical Review B 47(1), 558-561.

Lee, H., Park, Y.-K., Kim, S.-J., Kim, B.-H., Yoon, H.-S. and Jung, S.-C. (2016) Rapid degradation of methyl orange using hybrid advanced oxidation process and its synergistic effect. Journal of Industrial and Engineering Chemistry 35, 205-210.

Lee, S., Anwer, H. and Park, J.W. (2023) Oxidative power loss control in ozonation: Nanobubble and ultrasonic cavitation. J Hazard Mater 455, 131530.

Li, F., Xia, A., Guo, X.B., Huang, Y., Zhu, X.Q., Zhang, W.Y., Chen, R. and Liao, Q. (2023a) Photo-driven enzymatic decarboxylation of fatty acids for bio-aviation fuels production in a continuous

microfluidic reactor. Renewable & Sustainable Energy Reviews 183, 113507.
Li, J., Xie, G.Z., Jiang, J., Liu, Y.Y., Chen, C.X., Li, W.X., Huang, J.L., Luo, X.L., Xu, M., Zhang, Q.P., Yang, M. and Su, Y.J. (2023b) Enhancing photodegradation of Methyl Orange by coupling piezo-phototronic effect and localized surface plasmon resonance. Nano Energy 108, 108234.
Lughmani, F., Nazir, F., Khan, S.A. and Iqbal, M. (2022) Novel functionalized cellulose derivatives fabricated with Cu nanoparticles: synthesis, characterization and degradation of organic pollutants. Cellulose 29(3), 1911-1928.
Ma, Z., Melde, K., Athanassiadis, A.G., Schau, M., Richter, H., Qiu, T. and Fischer, P. (2020) Spatial ultrasound modulation by digitally controlling microbubble arrays. Nat Commun 11(1), 4537.
Monkhorst, H.J. and Pack, J.D. (1976) Special points for Brillouin-zone integrations. Physical Review B 13(12), 5188-5192.
Perdew, J.P., Burke, K. and Ernzerhof, M. (1996) Generalized Gradient Approximation Made Simple. Physical Review Letters 77(18), 3865-3868.
Rayaroth, M.P., Aravind, U.K. and Aravindakumar, C.T. (2016) Degradation of pharmaceuticals by ultrasound-based advanced oxidation process. Environmental Chemistry Letters 14(3), 259-290.
Rayaroth, M.P., Aravindakumar, C.T., Shah, N.S. and Boczkaj, G. (2022) Advanced oxidation processes (AOPs) based wastewater treatment - unexpected nitration side reactions - a serious environmental issue: A review. Chemical Engineering Journal 430, 133002.
Rickel, J.M.R., Dixon, A.J., Klibanov, A.L. and Hossack, J.A. (2018) A flow focusing microfluidic device with an integrated Coulter particle counter for production, counting and size characterization of monodisperse microbubbles. Lab Chip 18(17), 2653-2664.
Shanker, U., Rani, M. and Jassal, V. (2017) Degradation of hazardous organic dyes in water by nanomaterials. Environmental Chemistry Letters 15(4), 623-642.
Siddique, A., Meckel, T., Stark, R.W. and Narayan, S. (2017) Improved cell adhesion under shear stress in PDMS microfluidic devices. Colloids Surf B Biointerfaces 150, 456-464.
Sivanesan, J., Sivaprakash, B., Rajamohan, N., Phanindra, V.S.S., Sonne, C., Liew, R.K. and Lam, S.S. (2024) Remediation of tetracycline pollution using microplastics, green materials, membranes and sonocatalysts: a review. Environmental Chemistry Letters, 1-33.
Sun, X., Xu, D., Dai, P., Liu, X., Tan, F. and Guo, Q. (2020) Efficient degradation of methyl orange in water via both radical and non-radical pathways using Fe-Co bimetal-doped MCM-41 as peroxymonosulfate activator. Chemical Engineering Journal 402, 125881.
Thangavadivel, K., Konagaya, M., Okitsu, K. and Ashokkumar, M. (2014) Ultrasound-assisted degradation of methyl orange in a micro reactor. Journal of Environmental Chemical Engineering 2(3), 1841-1845.
Volk, A.A., Epps, R.W. and Abolhasani, M. (2020) Accelerated Development of Colloidal Nanomaterials Enabled by Modular Microfluidic Reactors: Toward Autonomous Robotic Experimentation. Advanced Materials 33(4), e2004495.
Wan, J., Bick, A., Sullivan, M. and Stone, H.A. (2008) Controllable Microfluidic Production of Microbubbles in Water-in-Oil Emulsions and the Formation of Porous Microparticles. Advanced Materials 20(17), 3314-3318.
Wang, J.L. and Wang, S.Z. (2020) Reactive species in advanced oxidation processes: Formation, identification and reaction mechanism. Chemical Engineering Journal 401, 126158.
Xiao, J.Y., Wang, M.Y., Pang, Z.J., Dai, L., Lu, J.F. and Zou, J. (2019) Simultaneous spectrophotometric determination of peracetic acid and the coexistent hydrogen peroxide using potassium iodide as the indicator. Analytical Methods 11(14), 1930-1938.
Xie, S., Huang, P., Kruzic, J.J., Zeng, X. and Qian, H. (2016) A highly efficient degradation mechanism of methyl orange using Fe-based metallic glass powders. Scientific Reports 6(1), 21947.
Xiu, W., Ren, L., Xiao, H., Zhang, Y., Wang, D., Yang, K., Wang, S., Yuwen, L., Li, X., Dong, H., Li, Q.,

Mou, Y., Zhang, Y., Yin, Z., Liang, B., Gao, Y. and Wang, L. (2023) Ultrasound-responsive catalytic microbubbles enhance biofilm elimination and immune activation to treat chronic lung infections. Sci Adv 9(4), eade5446.

Yuan, N., Zhang, G., Guo, S. and Wan, Z. (2016) Enhanced ultrasound-assisted degradation of methyl orange and metronidazole by rectorite-supported nanoscale zero-valent iron. Ultrason Sonochem 28, 62-68.

Yusuf, L.A., Ertekin, Z., Fletcher, S. and Symes, M.D. (2024) Enhanced ultrasonic degradation of methylene blue using a catalyst-free dual-frequency treatment. Ultrason Sonochem 103, 106792.